Frontal Lobe Function and Dysfunction, H. S. Levin, H. M. Eisenberg, A. L. Benton, Eds. (Oxford Univ. Press, New York, 1991), pp. 217]. See also P. R. Montague, P. Dayan, C. Person, T. J. Sejnowski, *Nature* **377**, 725 (1995). This action might occur both at the cortical level and in subcortical structures such as basal ganglia.

7. On the basis of a series of related studies [A. Bechara, D. Tranel, H. Damasio, S. W. Anderson, A. R. Damasio, *Soc. Neurosci. Abstr.* **21**, 1210 (1995); D. Tranel, A. Bechara, H. Damasio, A. R. Damasio, *ibid.* **22**, 1108 (1996)], we believe that the bias mechanism identified here is distinct from other neural mechanisms whose integrity is crucial for decision- making. Such mechanisms include response inhibition [J. M. Fuster, *The Prefrontal Cortex: Anatomy, Physiology, and Neuropsychology of the Frontal Lobe* (Raven, New York, ed. 3, 1996); R. Dias, T. W. Robbins, A. C. Roberts, *Nature* **380**, 69 (1996); A. Diamond, in *The Development and Neural Bases of Higher Cognitive Functions*, A. Diamond, Ed. (New York Academy of Sciences, New York, 1990), vol. 608, pp. 637–669], working memory [P. S. Goldman-Rakic, in *Handbook of Physiology; The Nervous System*, F. Plum, Ed. (American Physiological Society, Bethesda, MD, 1987), vol. 5, pp. 373–401], and selective attention [M. I. Posner and S. Dehaene, *Trends Neurosci.* **17**, 75 (1994)]. In other words, we propose an addition to mechanisms already recognized as necessary for proper reasoning rather than an alternative to those mechanisms.
8. A three-way analysis of variance (ANOVA) on the anticipatory SCRs generated by normal participants and patients (between group), during the pre-punishment and pre-hunch periods (within group), and in association with the bad and good decks (within group) revealed, most importantly, a significant two-way interaction of group with period [$F(1,14) = 16.24$, $P < 0.001$]. Subsequent Newman-Keuls tests on these SCRs revealed that, during the pre-punishment (baseline) period, the SCRs associated with the good or bad decks of normals or patients were not significantly different. However, there was a significant increase in the magnitude of these SCRs during the pre-hunch period, relative to the pre-punishment period, but only for normals ($P < 0.01$). The SCRs from normals during pre-hunch were also significantly higher than the SCRs of patients during both pre-punishment and pre-hunch ($P < 0.01$). Because all normals generated anticipatory SCRs, whereas all patients did not, Fisher's exact test, based on the hypergeometric distribution, yielded a one-sided $P < 0.001$. SCRs from normals who selected cards from the bad decks during the hunch period were compared to the SCRs associated with sampling the good decks. The same comparisons of SCRs were done for the conceptual period. Although SCRs from the bad decks during the hunch or the conceptual period were generally higher than those from the good decks, the difference did not reach statistical significance. However, Newman-Keuls tests comparing SCRs from the hunch or the conceptual period to those from the pre-punishment period revealed significant differences in the case of the bad decks ($P < 0.01$) but not the good decks. This suggests that SCR activity was sustained in the case of the bad decks, but may have been subsiding in the case of the good decks.
9. A similar ANOVA in which mean number of cards selected was used instead of SCRs revealed, most importantly, a significant three-way interaction of group with period with decks [$F(1,14) = 6.9$, $P < 0.02$]. With subsequent Newman-Keuls tests, the most relevant comparison was that patients selected significantly more cards from the bad decks relative to the good decks during the pre-hunch period ($P < 0.01$). By contrast, controls selected more from the good decks relative to the bad decks (the difference was not statistically significant). During the hunch and conceptual periods, controls selected significantly more cards from the good decks relative to the bad decks ($P < 0.01$). By contrast, patients still selected more cards from the bad decks relative to the good decks during the conceptual period (the difference was not statistically significant).
10. Supported by the National Institute of Neurological Diseases and Stroke grant PO1 NS19632.

29 October 1996; accepted 30 January 1997

Single Molecule Force Spectroscopy on Polysaccharides by Atomic Force Microscopy

Matthias Rief, Filipp Oesterhelt, Berthold Heymann, Hermann E. Gaub

Recent developments in piconewton instrumentation allow the manipulation of single molecules and measurements of intermolecular as well as intramolecular forces. Dextran filaments linked to a gold surface were probed with the atomic force microscope tip by vertical stretching. At low forces the deformation of dextran was found to be dominated by entropic forces and can be described by the Langevin function with a 6 angstrom Kuhn length. At elevated forces the strand elongation was governed by a twist of bond angles. At higher forces the dextran filaments underwent a distinct conformational change. The polymer stiffened and the segment elasticity was dominated by the bending of bond angles. The conformational change was found to be reversible and was corroborated by molecular dynamics calculations.

Recently a series of single molecule experiments provided detailed insight into intermolecular and intramolecular forces, providing relevant information on molecular mechanisms (*1*–*4*). In previous experiments we and others chemically linked molecular pairs such as biotin and avidin (*3*, *5*), or conjugated DNA strands (*6*), between the tip of an atomic force microscope (AFM) cantilever and support structures. Molecule-specific bond forces between binding pairs were measured upon separation and compared with known thermodynamic parameters (*4*). Here we used this approach to probe elastic properties of single polymer strands.

The experimental geometry is depicted in Fig. 1A. Dextrans (average molecular weight 500,000) linked to a gold surface through epoxy-alkanethiols were activated with one carboxymethyl group per glucose unit on average (*7*) and reacted with streptavidin such that several molecules were chemically bound to each dextran filament (Sensor Chip SA5, Pharmacia Biosensor AB, Uppsala, Sweden). The mean distance between the grafting points of two different polymer strands was about 200 Å, and the hydrated "polymer brush" extended 1000 to 2000 Å into the solution (*7*). Because in physiological buffer dextran behaves like an ideal polymer, the coil overlap is expected to be low. In our experiments streptavidin served as a molecular handle for the manipulation of the polymer to be investigated. An AFM cantilever with biotin bound to the AFM tip, following the protocol given in (*3*), was used to pull on individual dextran filaments through the biotin-streptavidin bond (*8*). To minimize the number of multiple bonds, which typically occur when the tip penetrates the polymer brush, we let the tip approach and retract step by step without it indenting into the sample until a binding event was registered. In this "fly fishing mode" the undesirable multiple bonds can be efficiently avoided (*9*). Alternatively, one can "manually" disentangle an individual filament from the polymer brush by slowly pulling back the tip while monitoring all multiple bonds and tangles rupturing until just one last filament is stretched (see the first trace of Fig. 4, discussed further below). This filament can then be repeatedly manipulated as long as the force is kept below the force limit of the molecular handles.

Several measured elongation curves of dextran strands of various lengths are shown in Fig. 1B (*10*). At the given extension rate of 0.5 μm/s the biotin-streptavidin bond is known to hold up to a force F of 250 ± 25 pN (*4*). The measured deformation curves were modeled by entropy springs with segment elasticity (*11*). Although the contour lengths $L_{contour}$ of the polymers varied from 0.4 to 1.6 μm, the measured Kuhn length $l_K = 6 \pm 0.5$ Å and the segment elasticity $k_{segment} = 670 \pm 100$ pN/Å showed only marginal variation between the filaments. This result was reproduced for several hundred filaments that were measured with different cantilevers in different experiments (*12*). The finding that the segment elasticity and Kuhn length are virtually identical for all measured dextran strands confirms that predominantly individual filaments are measured by this method and that the deformation of the couplers is negligible at polysaccharide lengths greater than 2000 Å (*13*).

An interpretation of the measured segment elasticity is given by molecular dynamics (MD) calculations. These reveal that at low forces the main contribution of the elasticity stems from a twist of the C5-C6 bond

M. Rief, F. Oesterhelt, H. E. Gaub, Lehrstuhl für Angewandte Physik, Ludwig-Maximilians-Universität, 80799 München, Germany.
B. Heymann, Theoretische Biophysik, Institut für Medizinische Optik, Ludwig-Maximilians-Universität 80333 München, Germany.

that results in an elongation of the filaments (Fig. 2A) (*14*). At forces less than 1000 pN this elongation is proportional to the force and gives rise to a segment elasticity of 750 pN/Å (Fig. 2B, black curve) (*15*). This value is in close agreement with the experimental result. At higher forces, however, our simulations revealed a discontinuity of the deformation caused by a flip of the C5-C6 bond. The simulation predicted a transition into a stiffer conformation with a segment elasticity of 3000 pN/Å (Fig. 2B, black curve).

To achieve these higher forces experimentally we introduced a different coupling mechanism. The loose ends of the grafted carboxymethylated dextran filaments (no streptavidin) were allowed to adsorb onto the AFM tip that had been made hydrophobic by silanization (*16*). Because this coupling protocol is based on a nonspecific interaction it is suitable only for homogeneous single component samples, but it gives rise to bond forces of more than 1000 pN. Extension curves that were recorded with the same tip at different spots of the sample and subsequently at the same spot of the sample are shown in Fig. 3, A and B, respectively. The traces in both figures exhibit the same deformation characteristics that we found at low forces for the biotin-streptavidin–coupled filaments (*17*). At 300 pN all traces show a horizontal deflection followed by an increase in slope, indicating a stiffening of the molecule as predicted qualitatively by the simulations. Typically the subsequent deformation curves from the same spot show a pronounced similarity. This is a strong indication that the AFM allows individual molecules to be addressed and permits repeated experiments with the identical molecule.

Extension curves of 20 different carboxymethylated dextran filaments with various contour lengths from 500 Å to 2 μm measured on different samples with different cantilevers were normalized according to their length and plotted in Fig. 3C (*18*). The superposition reveals that our description of the molecular deformation holds for filaments that differ in length by nearly two orders of magnitude. All elastic properties scale linearly with length, and all filaments show a transition at the same force. These observations clearly show that we are indeed stretching individual molecules of different length (*19*).

The transition in which carboxymethylated dextran is forced into the stiffer conformation starts at $F = 250 \pm 30$ pN and has a range of $\Delta F = 100 \pm 20$ pN (*20*). The segment elasticities are 670 pN/Å in the low force regime and 1700 pN/Å in the high force configuration. For a quantitative comparison with the MD simulations, which were carried out on native dextran, a set of single molecule force spectroscopy experiments was carried out with native dextran (Fig. 2B, dotted line). The segment elasticity in the low force regime (800 ± 100 pN/Å) is similar to the carboxymethylated dextran. In the high force conformation the elasticity is slightly higher (4000 ± 1000 pN/Å). The force range in which the dextran undergoes the conformational transition seems to be very sensitive to the carboxymethylation and is shifted from a range of 250 to 350 pN up to a range of 700 to 850 pN. The experimental and the calculated data are congruent with respect to both the elasticities and the width of the transition (0.6 Å) (Fig. 2B). However, the measured transition force is below the value predicted by theory. In view of the large differences between the experimental time scale, where the transition occurs within several hundredths of a second, and the computational time scale (fractions of a nanosecond), this difference can be explained and corroborated by the measured (*5*) and calculated (*21, 22*) rate dependence of the unbinding forces of molecular pairs like biotin and avidin.

To confirm that the measured transition is an elastic property of the molecular system, and to exploit the potential of this technique to continuously manipulate individual molecules, we repeatedly stretched a carboxymethylated dextran filament just below the rupture limit while the deformation was recorded. A sequence of subsequent traces recorded from an individual polymer is shown in Fig. 4. Note that in the first extension trace a few shorter filaments adhered to the tip and eventually detached. The evident full reversibility of the deformation traces shows that

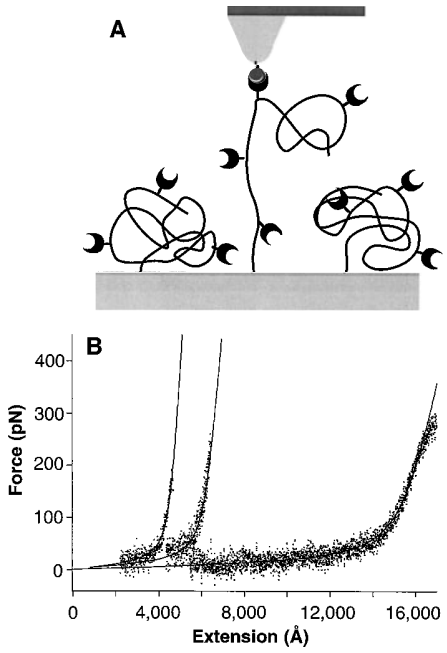

Fig. 1. (**A**) Schematics of molecular binding and polymer stretching. Dextran strands are chemically bound to a gold surface and are picked up by an AFM tip through a bond between streptavidin (half circles) and biotin (full circle). (**B**) Measured deformation curves of individual dextran filaments (dots) superimposed by a fit with an extended Langevin function (solid lines).

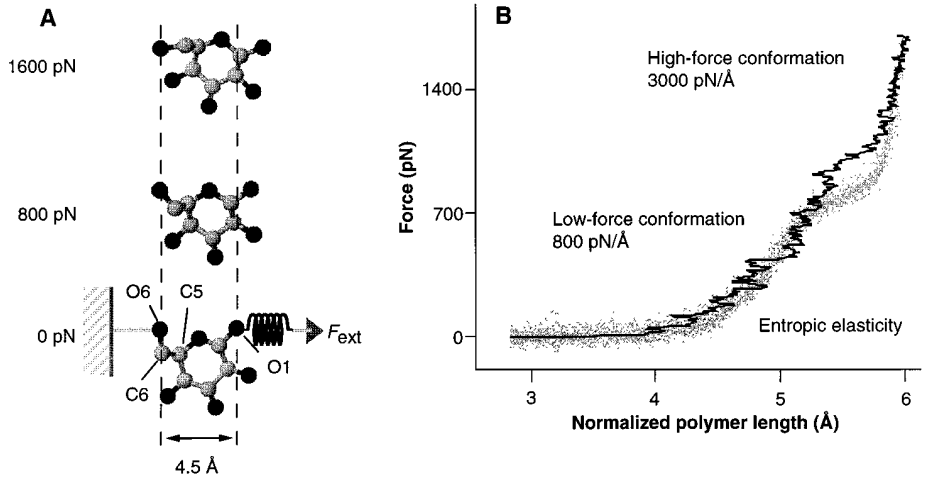

Fig. 2. Molecular dynamics calculations of the dextran deformation. (**A**) Ring conformations at different extension forces. (**B**) Normalized force versus elongation curve of a five-glucose unit of dextran in water calculated by MD simulations extended by entropic contributions (black curve). The grey dotted line is a superposition of 10 normalized curves (*18*) measured on native dextran. To correctly model the elasticity of the polymer and at the same time minimize computation time, we performed the calculations with a dextran strand consisting of five glucose units. The AFM experiment was simulated as closely as possible. The position of the O6 atom of the first monomer was kept fixed during the simulation. The cantilever spring acting on the other end of the molecule was represented by subjecting O1 of the last monomer to an additional potential $V_{spring} = k_c[z_{O1}(t) - z_{cant}(t)]^2/2$, the center of which was continuously shifted in the z direction by $z_{cant}(t) = z_{cant}(0) + v_{cant}t$ (*20*), where t is time. The spring constant k_c was chosen as 70 mN/m. As in the AFM experiment, the exerted force F_{ext} was measured by Hooke's law by observing the deflection $z_{O1}(t) - z_{cant}(t)$ of the lever. The pulling velocity v_{cant} was chosen as 0.25 Å/ps.

the transition is a nondissipative process. This finding confirms our interpretation of the plateau in the deformation curves of the dextran and signs it as a (at least in our time scale) purely elastic conformational change of the polysaccharide. The full reversibility indicates that the transition has only a low activation barrier and that the experiment is carried out under equilibrium conditions.

Single molecule force spectroscopy by AFM has proven to be a powerful addition to the nanoscopic piconewton toolbox. This technique that allows the controlled manipulation of individual molecules has revealed details of the molecular basis of the mechanical properties of polymers that could not be obtained otherwise. Whether this discovered discontinuous change in conformation, which is accompanied by an elongation of the molecule and followed by an increase in stiffness, has biological relevance remains speculation. One would, however, expect that such polymer characteristics significantly improve the polymer's ductility and may be a ubiquitous natural phenomenon.

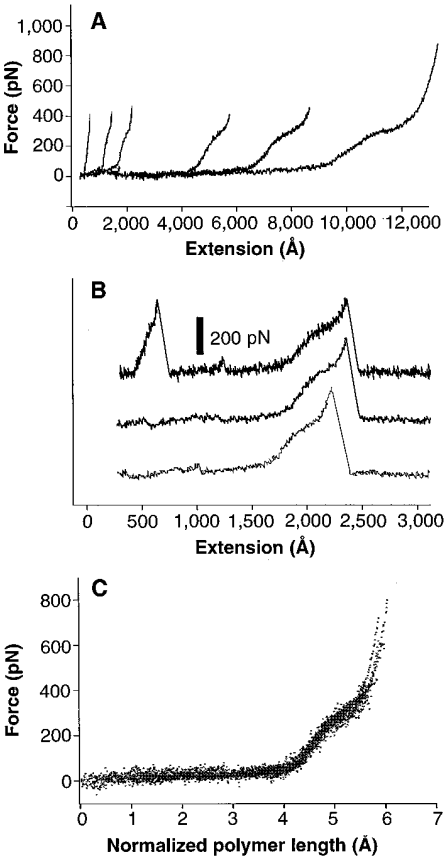

Fig. 3. Measured deformation curves of carboxymethylated dextran at higher forces (**A**) at different spots and (**B**) at the same spot. (**C**) Superposition of different normalized curves measured on different carboxymethylated samples.

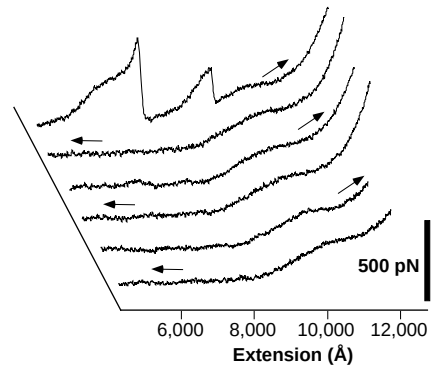

Fig. 4. Subsequent deformation curves, forcing an individual carboxymethylated dextran filament through the conformation transition. The measured deformation traces showed no visible hysteresis in the time scale of our experiments, therefore the curves were offset from trace to trace.

REFERENCES AND NOTES

1. S. B. Smith, Y. Cui, C. Bustamante, *Science* **271**, 795 (1996).
2. P. Cluzel *et al*., *ibid*., p. 792; T. T. Perkins, D. E. Smith, R. G. Larson, S. Chu, *ibid.* **268**, 83 (1995); M. Radmacher, M. Fritz, H. G. Hansma, P. K. Hansma, *ibid.* **265**, 1577 (1994); J. Käs, H. Strey, E. Sackmann, *Nature* **368**, 226 (1994); J. T. Finer, R. M. Simmons, J. A. Spudich, *ibid*., p. 113; K. Svoboda, C. F. Schmidt, B. J. Schnapp, S. M. Block, *ibid.* **365**, 721 (1993); U. Dammer *et al*., *Biophys. J.* **70**, 2437 (1996); P. Hinterdorfer, W. Baumgartner, H. J. Gruber, K. Schilcher, H. Schindler, *Proc. Natl. Acad. Sci. U.S.A.* **93**, 3477 (1996).
3. E.-L. Florin, V. T. Moy, H. E. Gaub, *Science* **264**, 415 (1994).
4. V. T. Moy, E. L. Florin, H. E. Gaub, *ibid.* **266**, 257 (1994).
5. G. U. Lee, D. A. Kidwell, R. J. Colton, *Langmuir* **10**, 354 (1994).
6. G. U. Lee, L. A. Chrisey, R. J. Colton, *Science* **266**, 771 (1994).
7. E. Stenberg, B. Persson, H. Roos, C. Urbaniczky, *J. Colloid Interface Sci.* **143**, 513 (1991).
8. Under conditions where the deformation of this molecular pair is less than that of the molecular couplers, the elongation of the entire system is dominated by the deformation of the couplers. The specific bond between molecular binding pairs may thus be used as a reversible coupling mechanism of a long and flexible molecule whose deformation is to be investigated.
9. This mode is particularly advantageous when the density of functional groups is high or when the polymeric material has a low density, such as in the outer layers of agarose beads used in earlier studies. On the dextran films used here the radius of the AFM tip is on the order of the mean distance of two grafted dextran coils. In this case an interaction of only a few polymer strands with the tip is likely. A noncommercial AFM, customized for force measurements, was used to do the experiments. Piezo nonlinearities were corrected with a strain gauge. The spring constants of the cantilevers (Digital Instruments, Santa Barbara, CA) were calibrated by measuring their thermal excitation (*23*). Measured values ranged from 25 to 120 mN/m. All experiments were carried out in phosphate-buffered saline (150 mM NaCl, pH 7.4).
10. Because the streptavidin molecules are distributed statistically along the polysaccharide chain, it is very likely that the tip does not pick up the end of the chain. Because the dextran is only branched and not cross-linked, the free end is dangling, and as a result, the apparent length of the polymer is reduced.
11. Following Smith *et al*. (*1*), the Langevin function was extended by a segment elasticity $k_{segment}$:

$$x(F) = \left[\coth\left(\frac{Fl_K}{k_BT}\right) - \frac{k_BT}{Fl_K}\right]\left[L_{contour} + \frac{nF}{k_{segment}}\right]$$

$L_{contour}$ is the length of the completely stretched filament. The Kuhn length l_K is the length of the statistically independent segments in the freely jointed chain model, n is the number of monomers in the filament, T is the temperature, and k_B is Boltzmann's constant. Here both n and the segment elasticity $k_{segment}$ are related to monomers and not to the Kuhn segments. In order to fit the data by this model, it was assumed that the point of zero extension is where the tip meets the hard substrate.
12. M. Rief, F. Oesterhelt, B. Heymann, H. E. Gaub, data not shown.
13. It is very likely though, that by pulling at one end of the coiled polymer while keeping the other end fixed, we do tighten random knots. The measured scaling of the elastic properties of the polymer indicates that these knots are compact and do not contribute significantly to the elasticity of the polymer. Whether or not these knots disentangle upon expansion is not known yet. A marked contribution from the interchain interaction can also be excluded. In the extension regime, where a measurable tension is built up in the polymer, the largest part of the extended polymer is far out of reach of the other poymers of the brush.
14. Equilibration (300 K) and pulling simulations were done with the program EGO (*24*), which uses the CHARMM force field (*25*). For modeling and minimization of the structure containing five glucose units, the program QUANTA (Molecular Simulations, Waltham, MA) was used. All simulations were done in water.
15. Unlike the measured data of long dextran chains, the MD calculations of a five-glucose unit of dextran do not reflect entropic contributions in the low force regime below 200 pN. The calculated elasticity was therefore extended by entropic contributions in the following way: The linear segment elasticity extension $k_{segment}$ of the Langevin function (*11*) was replaced by the calculated elasticity and normalized (*18*).
16. The cantilevers were silanized in dimethyl-dichlorosilane (Sigma, Deisenhofen, Germany) vapor and rinsed with acetone. Commercially available carboxymethylated dextran films on gold (Sensor Chip CM5, Pharmacia Biosensor AB, Uppsala, Sweden) were used as samples in order to be able to compare the results to the similarly treated but streptavidin-functionalized dextrans used before.
17. A fit of the low force regime results in the same Kuhn length and segment elasticity as found in Fig. 1.
18. The polymer extension was divided by the contour length and multiplied with the length of the monomer. This normalization allows the comparison between the force profiles of dextran filaments of different lengths.
19. Obviously contributions to the elastic properties due to interchain interactions do not play a measurable role in our experiment. Interchain interactions as well as nonlocal intrachain interactions like complex knots would scale nonlinearly and would not result in the observed strict linear scaling with length.
20. When measured with the same cantilever the variation of these values is $<5\%$ so that the transition is now routinely used for internal force calibration.
21. H. Grubmüller, B. Heymann, P. Tavan, *Science* **271**, 997 (1995).
22. A decrease of the transition force with the pulling velocity could also be observed in our dextran simulations.
23. E. L. Florin *et al*., *Biosens. Bioelectronics* **10**, 895 (1995).
24. M. Eichinger, H. Grubmüller, H. Heller, *User Manual for EGO_VIII, Release 2.0* (Theoretische Biophysik, Institut fuer Medizinische Optik, Universität Muenchen, 1995).
25. B. R. Brooks *et al*., *J. Comp. Chem.* **4**, 187 (1983).

26. Supported by the Deutsche Forschungsgemeinschaft and a Max-Planck research award. We gratefully acknowledge helpful discussions with P. Tavan, H. Grubmüller, M. Ludwig, and S. Lofas and inspiring advice from J. I. Brauman.

4 September 1996; accepted 5 December 1996